Modulated Fluorescence Correlation Spectroscopy with Complete Time Range Information

Gustav Persson, Per Thyberg, and Jerker Widengren
Experimental Biomolecular Physics, Department of Applied Physics, Royal Institute of Technology, AlbaNova University Center, Stockholm, Sweden

ABSTRACT Two methods to combine fluorescence correlation spectroscopy (FCS) with modulated excitation, in a way that allows extraction of correlation data for all correlation times have been developed and experimentally verified. One method extracts distortion-free correlation data from measurements acquired with standard hardware correlators provided the fluorescence does not change systematically within the excitation pulses. This restriction does not apply to the second method, which, however, requires time-resolved acquisition of the fluorescence intensity. Modulation of the excitation in an FCS experiment is demonstrated to suppress triplet population buildup more efficiently than a corresponding reduction in continuous wave excitation intensity (shown for the dye rhodamine 6G in aqueous solution). Excitation modulation thus offers an additional means to optimize the FCS measurement conditions with respect to the photophysical properties of the dyes used. This possibility to suppress photoinduced states also provides a useful tool to distinguish additional processes occurring in the same time regime in the FCS measurements, as demonstrated here for the protonation kinetics of fluorescein at different pH. In general, the proposed concept opens for FCS measurements with a complete correlation timescale in a range of applications where a modulated excitation is either necessary or brings specific advantages.

INTRODUCTION

Fluorescence correlation spectroscopy (FCS) (1) is a versatile method for characterizing the dynamics of a low number of fluorescent molecules moving through a very small detection volume, normally the laser focus in a confocal microscope. It is used in numerous biophysical studies and has many applications in analytical chemistry and biochemistry (see the literature (2–7) for introductions and reviews). A range of molecular dynamic processes that affect the fluorescence intensity may be monitored by FCS. However, a common complication is that several processes take place in the same time regime, making them difficult to separate. Many of the best fluorescent markers, synthetic organic dyes as well as fluorescent proteins, exhibit flickering due to, e.g., triplet formation (8), *trans-cis* isomerization (9), electron transfer (10), or protonation (11). Whereas each of these processes may be exploited to probe the environment, sometimes they complicate FCS measurements or data analysis by obscuring a process of interest falling within the same time range. It has previously been shown that the amount of triplet formation may be controlled by modulating the excitation, with pulse widths and periods in the range of the transition times of the involved states (12). This should also be true for other photoinduced processes, i.e., all of the processes mentioned above, except the concentration-dependent protonation process. Given the role of the triplet state as a precursor state of photobleaching (13,14), suppression of the triplet state by, e.g., chemical means has proven useful as a way of decreasing the photobleaching of fluorescent dyes (fluorophores) (15). For pulsed excitation with pulse widths in the subnanosecond time range, it has accordingly been shown that by increasing the pulse separation beyond that of the triplet state relaxation time and thereby allowing full triplet state relaxation between the pulses, immobilized fluorophores can emit 10–20 times more photons before they bleach (16). Consequently, in view of the importance of molecular fluorescence brightness and quantum yield in FCS, the incorporation of modulated excitation ought to be of interest in many FCS experiments. However, modulating the excitation in FCS measurements also introduces complications. It induces periodic ringing in the correlation curve, making a direct interpretation difficult. If the modulation parameters (pulse width and period) are not chosen with care the modulation even destroys the correlation information for certain time regimes.

In this work we introduce and experimentally verify a concept for the retrieval of the complete correlation curves from FCS measurements with modulated excitation having an arbitrarily low fraction of active excitation. Following the experimental verification of the approach itself, the usefulness of the modulated FCS concept is demonstrated in two examples. First, we show, for the common fluorescent dye rhodamine 6G (Rh6G) in water, that modulated excitation can be applied to FCS experiments to suppress the triplet buildup more efficiently than by reducing excitation power with continuous wave (CW) excitation.

Second, it is shown how the modulated FCS concept can be used for protonation kinetics measurements of fluorescein at different pH, providing an example of how suppression of the triplet state population significantly

Submitted May 28, 2007, and accepted for publication September 13, 2007.

Address reprint requests to Jerker Widengren, E-mail: jerker@biomolphysics.kth.se.

Editor: Petra Schwille.

0006-3495/08/02/977/09 $2.00

doi: 10.1529/biophysj.107.113332

facilitates the analysis of a kinetic process, generating fluorescence blinking in the same time range as the triplet state kinetics.

In general, and in addition to the examples shown in this work, the proposed method should make it possible to perform FCS measurements with a complete correlation timescale in a range of applications where a modulated excitation is either necessary or brings specific advantages. An outline of such additional applications is given in the concluding section of this work.

THEORY

In fluorescence correlation spectroscopy information is extracted by calculation of the normalized autocovariance of the fluorescence signal $I(t)$:

$$G(\tau) = \frac{\langle I(t)I(t+\tau)\rangle}{\langle I(t)\rangle\langle I(t+\tau)\rangle}. \quad (1)$$

Here the brackets denote averaging over the time t with τ being the lag time or correlation time. $G(\tau)$ reports on the characteristic time of the process being studied and the number of fluorescent entities taking part in this process. For studies of fast processes the dead time of the detector has to be circumvented. This is usually achieved by splitting the fluorescence onto two separate detectors in a so-called Hanbury-Brown and Twiss setup (17) and calculating the cross correlation of the two signals:

$$G(\tau) = \frac{\langle I_1(t)I_2(t+\tau)\rangle}{\langle I_1(t)\rangle\langle I_2(t+\tau)\rangle}. \quad (2)$$

This has the additional benefit of relieving the correlation curve of effects of detector afterpulsing.

In the following, two approaches for retrieving a correlation curve for a modulated measurement are presented. The second is a generalization of the first and more generally applicable, whereas the first has the advantage of being useful with conventional correlators. To improve the readability the correlation function of Eq. 2 is hereafter denoted as an autocorrelation, and the denominator is simplified to the square of the mean intensity $\langle I\rangle^2$, although cross correlation of two detection channels and symmetric normalization were used in practice.

Filtering by modulation correlation

If the detected intensity is assumed linearly dependent on the intensity of the modulated excitation (a situation analogous to modulation of the light emitted from the sample), it can be expressed as a product of two uncorrelated components, the modulation M and the fluorescence F:

$$I(t) = M(t)F(t). \quad (3)$$

The autocorrelation function, $G_I(\tau)$, of the detected intensity can in this case be expressed as

$$G_I(\tau) = \frac{\langle I(t)I(t+\tau)\rangle}{\langle I\rangle^2} = \frac{\langle M(t)F(t)M(t+\tau)F(t+\tau)\rangle}{\langle MF\rangle^2} = \frac{\langle M(t)M(t+\tau)\rangle\langle F(t)F(t+\tau)\rangle}{\langle M\rangle^2\langle F\rangle^2}, \quad (4)$$

where the last equality follows from M and F being uncorrelated. For all τ where $\langle M(t)M(t+\tau)\rangle \neq 0$ we can get the autocorrelation function of F by dividing the autocorrelation $G_I(\tau)$ of the detected intensity with that of the modulation, $G_M(\tau)$:

$$G_F(\tau) = \frac{\langle F(t)F(t+\tau)\rangle}{\langle F\rangle^2} = \frac{\langle I(t)I(t+\tau)\rangle}{\langle I\rangle^2} \Big/ \frac{\langle M(t)M(t+\tau)\rangle}{\langle M\rangle^2} = \frac{G_I(\tau)}{G_M(\tau)}. \quad (5)$$

This method can easily be used with normal hardware correlators. Measuring reflected excitation light to get the required correlation function for the modulation, $G_M(\tau)$, allows extraction of $G_F(\tau)$ from the measured intensity correlation function $G_I(\tau)$ by means of Eq. 5.

Filtering by time-shifted fluorescence correlation

In a more general case the intensity trace collected during a measurement with modulated excitation can be considered a product of three components:

$$I(t) = M(t)V(t)F(t). \quad (6)$$

Here M is the excitation modulation and F corresponds to the fluorescence of the observed molecules, as if they where continuously illuminated, but with a molecular brightness determined by the average state population distribution during the excitation pulses. V is a factor taking care of the variations in fluorescence during the pulses due to the modulated excitation. Hence, V is to a first approximation periodic, with the same period T_p as the modulation. The autocorrelation of the measured intensity can be expressed as

$$\frac{\langle I(t)I(t+\tau)\rangle}{\langle I\rangle^2} = \frac{\langle M(t)V(t)F(t)M(t+\tau)V(t+\tau)F(t+\tau)\rangle}{\langle MVF\rangle^2} = \frac{\langle M(t)V(t)M(t+\tau)V(t+\tau)\rangle\langle F(t)F(t+\tau)\rangle}{\langle MV\rangle^2\langle F\rangle^2}. \quad (7)$$

Taking advantage of the periodic nature of the excitation and fluorescence variations a modulation filter function can be introduced to remove the periodic characteristics of the correlation function. This filter function can be generated by introducing a lag-time shift NT_p, which is a multiple N of the modulation period T_p and much larger than the characteristic

time of any process contributing to the correlation (except the modulation). In the case of fluorescent molecules diffusing freely through the detection volume the lag-time shift has to be much larger than the diffusion time τ_D ($NT_p \gg \tau_D$):

$$\frac{\langle I(t)I(t+NT_p+\tau)\rangle}{\langle I\rangle^2} = \frac{\langle M(t)V(t)M(t+NT_p+\tau)V(t+NT_p+\tau)\rangle}{\langle MV\rangle^2\langle F\rangle^2}\overbrace{\langle F(t)F(t+NT_p+\tau)\rangle}^{=\langle F\rangle^2} = \frac{\langle M(t)V(t)M(t+\tau)V(t+\tau)\rangle}{\langle MV\rangle^2}. \quad (8)$$

$\langle F(t)F(t+NT_p+\tau)\rangle$ reduces to $\langle F\rangle^2$ because NT_p is larger than the times of any correlations in F and hence the factors are totally uncorrelated. Dividing the initial correlation function of Eq. 7 with the filter function of Eq. 8 gives the autocorrelation of F:

$$\frac{\dfrac{\langle I(t)I(t+\tau)\rangle}{\langle I\rangle^2}}{\dfrac{\langle I(t)I(t+NT_p+\tau)\rangle}{\langle I\rangle^2}} = \frac{\langle F(t)F(t+\tau)\rangle}{\langle F\rangle^2} = G_F(\tau). \quad (9)$$

This operation can only be carried out for the lag times where the filter function has a nonzero value. This puts some demands on the modulation pulse train if a complete correlation function is to be deduced.

Pulse trains to achieve complete correlation curves

A great benefit of FCS is that it provides dynamic information over a vast continuous time range. To provide correlation information for all time regimes in FCS measurements with modulated excitation the excitation must be such that fluorescence photons can occur in pairs separated by any time shorter than the measurement duration. For a regular rectangular shaped pulse train, with one pulse per modulation period T_p, the pulse width w_p must be at least half a period to fulfill this. Such a pulse train, with a pulse width that is exactly half the period, has a duty cycle of 50%. The duty cycle is normally defined as the ratio of the pulse width and the period, whereas here, for our more complex pulse trains, we choose to define it analogously as the fraction of the total time the excitation is actually active.

To achieve duty cycles <50% we designed pulse trains with multiple pulses per modulation period. Based on a rectangular pulse train with 50% duty cycle, pulse trains with arbitrarily small duty cycles can be generated by recursively removing the middle third of each pulse. These will still contain information on all timescales, limited only by the resolution of the detection system. Accordingly, the number of pulses per modulation period is doubled for each recursion. A more general realization of the same idea would be to recursively remove the n even $1/(2n+1)$ parts (n positive integer) of each pulse, changing the duty cycle by a factor of $(n+1)/(2n+1)$ for each recursion (Fig. 1). The duty cycle η for a given parameter n and number of recursions r is thus given by:

$$\eta(n,r) = \frac{1}{2}\left(\frac{n+1}{2n+1}\right)^r. \quad (10)$$

Table 1 gives an overview of duty cycles for the lowest values of n and r. The approach already described corresponds to $n = 1$.

Weighting

The correlation function (Eq. 1) for each lag time is essentially the ratio of the number of occurring photon pairs, with time between the photons within a certain interval, and

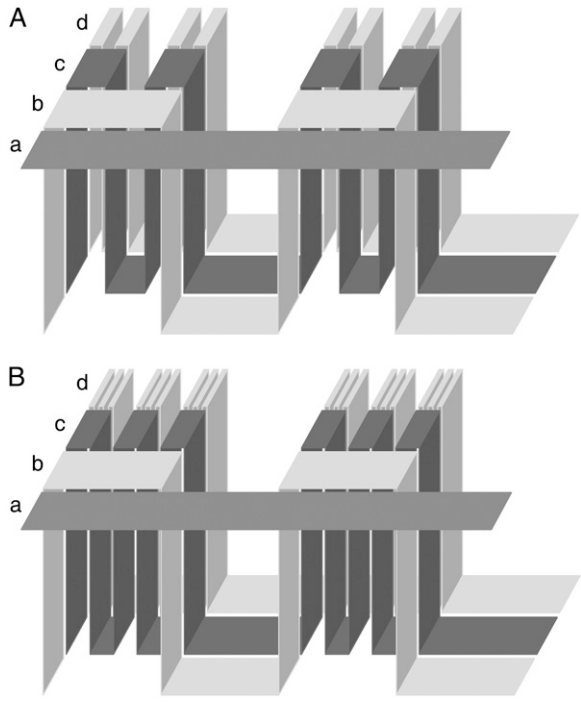

FIGURE 1 (*A*) Design of lower duty cycle pulse trains, allowing extraction of complete correlation curves, by starting with a 50% duty cycle square wave and recursively removing the middle third of each pulse. Ribbon *a* represents CW excitation, *b* is a 50% duty cycle square wave, *c* and *d* show the two first recursion steps. (*B*) Illustration of the more general approach, removing the n even $1/(2n+1)$ parts. Here $n = 2$.

TABLE 1 Pulse train duty cycles

	Duty cycle (%)			
Recursions	$n = 1$	$n = 2$	$n = 3$	$n = 4$
0	50.0	50.0	50.0	50.0
1	33.3	30.0	28.6	27.8
2	22.2	18.0	16.3	15.4
3	14.8	10.8	9.3	8.6
4	9.9	6.5	5.3	4.8

Duty cycles for a range of pulse trains providing full-time range correlation information. Rows correspond to different numbers of recursions and the columns to different values of the parameter n, which defines the number of $1/(2n + 1)$ parts of every pulse to be removed for each recursion. The duty cycle is here defined as the fraction of time for which the excitation is active.

the product of the total number of photons in the detection channels. Modulating the excitation influences the number of photon pairs contributing to certain points in the correlation curve more than others. This means, e.g., that the correlation for lag times corresponding to odd multiples of the pulse width (in a pulse train designed as described above) will be noisier than the rest of the curve, i.e., contain less information. To take this into account when fitting analytical models to the correlation curves a weighting scheme was introduced.

A commonly used weighting for FCS measurements with CW excitation is the one introduced by Koppel (18). He expressed the standard deviation for the correlation function in terms of average number of photons per time bin, i.e., average fluorescence intensity, and number of bin pairs multiplied and summed up for each correlation channel. This is, however, not applicable when the excitation is modulated, introducing periodic variations in the fluorescence intensity. Hence, a new weighting was derived based on the assumption that detected photons are generated by a Poissonian process (19). The standard deviation for each point in the correlation curve for a modulated measurement was estimated as:

$$\sigma(G_F(\tau)) = G_F(\tau)\sqrt{\frac{1}{N_{p,D}(\tau)} + \frac{1}{N_{1,D}} + \frac{1}{N_{2,D}} + \frac{1}{N_{p,S}(\tau)} + \frac{1}{N_{1,S}} + \frac{1}{N_{2,S}}}, \quad (11)$$

where the $N_{i,j}$ denote either the number of photon pairs (for $i = p$) with interphoton times within an interval around τ, or the total number of photons in channel i ($i = 1$ or 2) used for calculating either the direct correlation of the modulated measurement ($j = D$) or the filter function ($j = S$). As a first approximation $N_{i,j}$ were assumed independent of each other. See Appendix I for the full derivation.

MATERIALS AND METHODS

Instrumental setup

A homebuilt confocal setup, consisting of an Olympus IX-70 microscope body and a linearly polarized Ar-ion laser (Carl Zeiss, Jena, Germany, rebuilt by LASOS Laser-Fertigung GmbH, Jena, Germany) operated at 514.5 nm, was used for the measurements. An acoustooptic modulator (AOM) (AA.MT.200/A0,5-VIS, AA Opto-Electronic, Orsay, France) was inserted into the excitation beam path to modulate the laser intensity. The laser beam was focused into the sample by a 60×, NA 1.2, UPlanApo Olympus objective. Emitted fluorescence was collected by the same objective, separated from the excitation light by a dichroic mirror and focused by a 150-mm achromatic lens onto a pinhole of 30 μm diameter in the image plane, after recollimation split by a 50/50 beam-splitter cube, and finally detected by two avalanche photodiodes (APDs) (SPCM-AQR-14/16, PerkinElmer Optoelectronics, Fremont, CA). Rayleigh- and Raman-scattered excitation light was suppressed by use of band-pass filters in front of each APD (HQ565/75, Chroma Technology, Rockingham, VT).

During measurements, excitation powers were measured directly after the acoustooptic modulator. The power reaching the sample through the objective has been measured to ~56% of these values. Presented excitation powers correspond to light incident on the sample. Excitation powers for modulated measurements refer to the power during an excitation pulse.

The rise and fall time of the pulses of the modulated laser excitation was measured by a photodiode (PHD 400, Becker & Hickl GmbH, Berlin, Germany), connected to a 500-MHz digital oscilloscope (TDS 3052, Tektronix, Beaverton, OR), to a value <10 ns, in agreement with the AOM specifications.

To determine the shape of the excitation pulses, time-resolved data traces of scattered light from a water sample were recorded by use of the instrumentation above. Integration over the pulses has shown that the energy content of a pulse corresponds to a rectangular pulse ~2 ns shorter than the value set by the modulator controller.

For generation of excitation-light-based filter functions, $G_M(\tau)$, according to Eq. 5, the objective was replaced by a mirror and the emission band-pass filters by a neutral density filter to give a sufficient signal/noise ratio.

Data collection and processing

Data was collected using a PCI-6602 counter/timer card (National Instruments, Austin, TX), counting pulses from the internal clock between each pair of consecutive photons detected by the APD connected to a counter, rendering separate time-tagged photon traces with a resolution of 12.5 ns for each channel. The modulator driver was externally controlled by a digital signal generated by the same card. For the more complex pulse trains two cards of the same type, interconnected over the built-in RTSI bus, were used to generate the control signal. All modulated measurements presented in this work were done with pulse trains generated according to the scheme described in the Theory section, with $n = 1$. Pulse generation was controlled by the same card used for data acquisition to avoid errors in the time shift introduced in Eq. 8, which could be caused by timing discrepancies between two separate devices. The internal 80-MHz clock of the card was used as time base. A program was written in LabView to acquire the data and control the modulator.

Measurements were also made with an ALV-5000/E correlator (ALV-GmbH, Langen, Germany), with an ALV 5000/FAST Tau Extension board giving a 12.5-ns lag-time resolution when cross correlating between channels.

Correlation of the time-tagged photon traces was accomplished by a C-program, written in-house based on the algorithm presented by Laurence et al. (20). This program also contained functionality for introducing the large offsets necessary for calculating the modulation filters according to Eq. 8. For the measurements presented in this work an offset of ~300 ms was used. For division of correlation functions and other minor operations built-in Linux command line tools were used.

To make use of the full signal/noise ratio within the excitation pulses, photons arriving when excitation is turned off can be filtered out by software gating. For this, histograms were generated in a small LabView program to show the distribution of photons arriving at different times within each modulation cycle. Histogram bins with a low accumulated number of photons thus represented times between excitation pulses. Rejection of photons falling into bins with a number of photons below a set threshold

value provided a simple method for suppressing signal from times without excitation. For the measurements in this study, the effects of gating were negligible, because of low detector dark counts and good measurement conditions. For measurements with low excitation duty cycles and high ambient background gating would however be an attractive option. In this case most of the background was due to scattered excitation light. Suppression of this by software gating (21) was not applicable because the excitation pulses were longer than the fluorescence lifetime.

Sample preparation

Rhodamine 6G (Fluka Chemie AG, Buchs, Switzerland) and fluorescein (Sigma-Aldrich, St. Louis, MO) were dissolved in ethanol to give stock solutions with concentrations of 10 μM. The Rh6G stock solution was diluted in ultrafiltrated (Easypure, Wilhelm Werner GmbH, Leverkusen, Germany) water to a concentration of $\sim$1 nM. Phosphate buffer stock solutions (100 mM) were prepared by diluting different amounts of acid and base components ($NaH_2PO_4{\cdot}H_2O$, Merck KGaA, Darmstadt, Germany and $Na_2HPO_4{\cdot}2H_2O$, Fluka Chemie AG, Buchs, Switzerland, respectively) in water to give different pH (6.0 and 9.4). The high pH is outside the buffering range but serves to ensure a very low amount ($<$0.2%) of protonated fluorescein in the sample. Fluorescein stock solution was diluted to $\sim$10 nM in a mixture of buffer stock solution and water yielding two samples with 1 mM low pH buffer and 10 mM high pH buffer, respectively.

Typically, 5 ml of each sample was put in a closed container to avoid intensity drift due to evaporation or photobleaching.

RESULTS AND DISCUSSION

Correlation curves from measurements with modulated excitation

Measurements were made on a Rh6G sample, both with a hardware multi-tau correlator and time-tagged photon trace collection, to demonstrate the ability of the described approaches to generate distortion-free correlation curves from measurements with modulated excitation.

Fig. 2 *A* shows two measurements with two different excitation pulse trains applied, analyzed with the ALV-5000 correlator. Here filtering was performed according to Eq. 5 by dividing the correlation curves by the correlations of the corresponding measurements on reflected light. Insets show unfiltered correlation curves and their corresponding filter functions. The two pulse trains had the same period and pulse width comparable to or much longer than the triplet relaxation time ($\tau_T \approx 1.5$ μs). This method gives essentially distortion-free data for excitation with short pulses, because the fluorescence intensity does not change significantly during each pulse, i.e., $V(t)$ is approximately constant and Eq. 7 reduces to Eq. 4. For longer excitation pulses, spikes are observed in the correlation curve around lag times corresponding to odd multiples of the pulse width. The reason for this is that the fluorescence decay within the pulses due to triplet population buildup constitutes a periodic contribution to the signal not taken into account by the filter function applied here. To confirm this, several measurements, with different modulation parameters and different excitation powers, as well as simulations were performed. These consistently showed that the amplitude of the spikes decreases with decreasing triplet population. In Fig. 2 *B* measurements are shown, where the data were collected as time-tagged photon traces and software-correlated. Here, the modulation filtering was done by dividing the correlation curves by the time-shifted correlation function of the same measurements, as described above (Eq. 9). Both of these curves are well-behaved, and the fluorescence decay during the pulses is no longer a problem. An additional major advantage of this method is that it only requires one measurement to generate a filtered correlation curve. In contrast to the first method, no separate determination of the autocorrelation function of the modulation is needed. This makes the latter approach more robust and less sensitive to changes in the experimental setup. For these reasons, this method was used for all the following measurements presented in this work.

To show that the modulated FCS concept also works with pulse widths and gaps in the excitation pulse train on the order of the diffusion time and longer, measurements were made with a period of 162 μs. Fig. 2 *C* shows a comparison between a CW measurement (*solid line*) and two modulated measurements with pulse widths 81 μs (*dashed line*) and 3 μs (*dotted line*). The curves are all very similar, although, as expected, the one corresponding to the measurement with the shorter pulses lies slightly above the others in a range around 10 μs. This is caused by a reduced triplet population due to the shorter pulses (12). The decreased saturation effect on the spatial distribution of the detected fluorescence intensity following the reduction of the triplet population generates an apparently smaller detection volume. The average number of molecules in the detection volume thus decreases and the amplitude of the part of the correlation curve attributable to diffusion is increased (8,22). This effect systematically occurs throughout our data. The decreased triplet population coincidentally makes the total correlation amplitude for short lag times essentially the same as for the other curves.

Additionally, artificial square and sine wave modulations were applied to a CW measurement to verify that the method itself does not distort the correlation curve. This is shown in Fig. 2 *D*. The correlation curves of the artificially modulated measurements became a bit noisier because of the reduced amount of data, but no significant systematic deviations were observed.

Efficient triplet suppression

A series of measurements were made on Rh6G with different modulation parameters and compared with a power series with CW excitation. To clearly illustrate the decreased triplet population buildup by modulated excitation the relatively high peak excitation power of 0.84 mW was chosen for the modulated measurements. Fig. 3 *A* shows a CW measurement with 0.84 mW excitation compared with two modulated measurements. The average triplet population clearly decreases with shorter pulses and the decreasing saturation effect gives rise to a higher amplitude of the diffusion

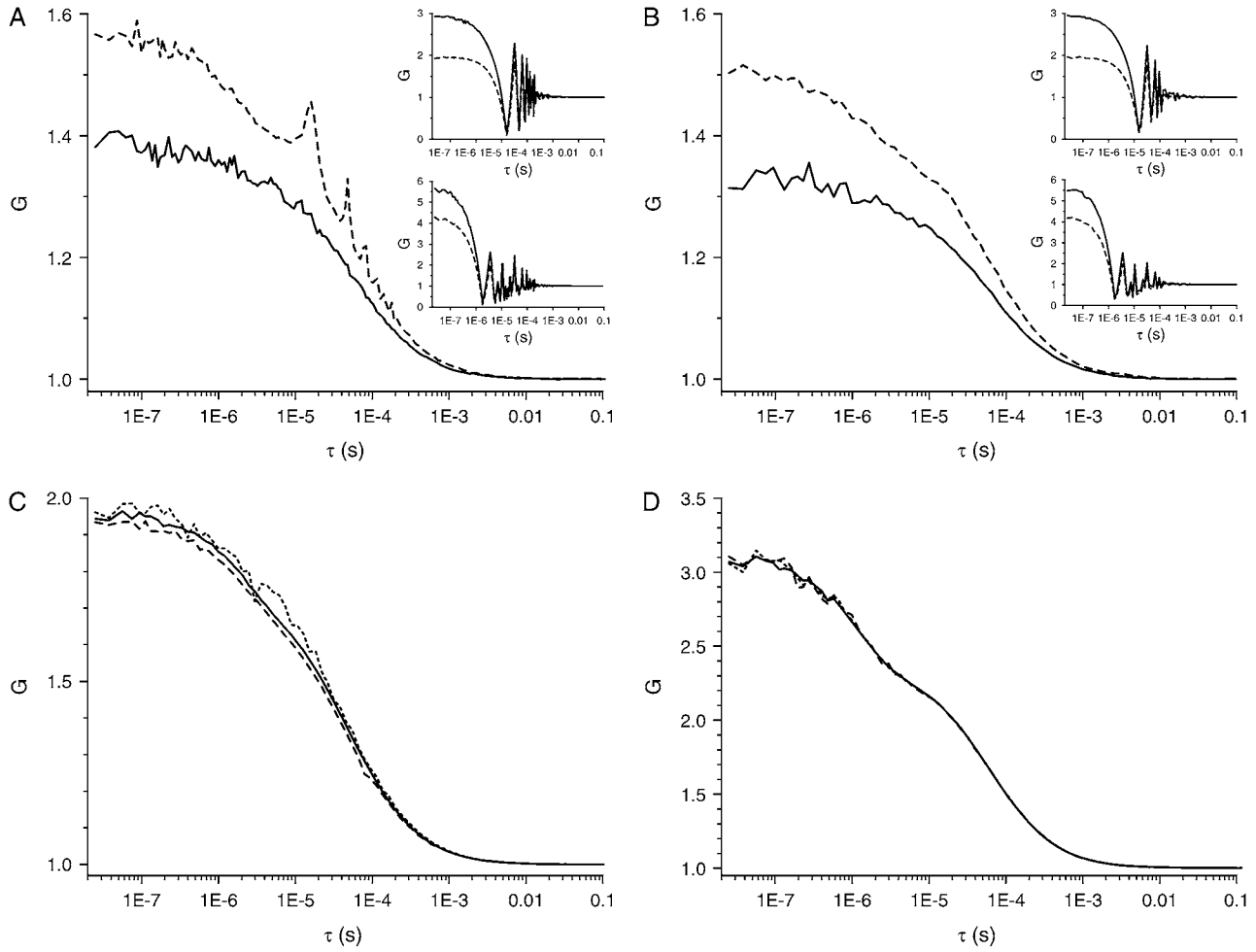

FIGURE 2 (*A*) Measurements on Rh6G, made with an ALV-5000 correlator. Curves generated by dividing correlation curves for the Rh6G measurements with modulated excitation by curves from measurements on reflected excitation light with corresponding modulation. Pulse widths in the excitation pulse trains were 1.8 (*solid curve*, modulation parameters $n = 1$ and $r = 2$) and 16.2 μs (*dashed curve*, $n = 1$, $r = 0$). The modulation period was 32.4 μs for both measurements and the excitation power during pulses was 0.28 mW. Insets show the unfiltered correlation functions (*solid curves*) and the corresponding filter functions (*dashed curves*). The upper inset corresponds to the measurement with the longer pulses. (*B*) Measurements corresponding to those in panel *A* but software correlated after collection of time-tagged photon traces. The filter functions, by which the correlation functions of the modulated measurements have been divided to yield these curves, were generated by introducing a time shift between the data channels before correlating as described in the Theory section. Insets as in panel *A*. (*C*) A CW measurement (*solid curve*) compared with modulated measurements with period 162 μs and pulse widths 81 μs (*dashed curve*, $n = 1, r = 0$) and 3 μs (*dotted curve*, $n = 1, r = 3$). The excitation power was 0.17 mW. (*D*) A CW measurement (*solid curve*) compared with correlation curves based on the same measurement but with artificial modulations added after measurement. The dashed curve represents data with a sine modulation with 10-μs period and the dotted curve shows the result after imposing a square wave modulation on the data, having a 5-μs pulse width and a 10-μs period. (In the measurements on which figures *A* and *B* are based no measures were taken to control the concentration since the main interest was the general appearance of the correlation curves. The differences in correlation amplitude are attributable to differences in concentration between the individual measurements.)

component of the correlation curve. The saturation effect referred to here is the flattening of the fluorescence intensity profile due to triplet population buildup in the center of the laser focus and the resulting apparent enlargement of the Gaussian detection volume (8,22). The triplet parameters were determined by nonlinear least-squares fits of the model (23):

$$G(\tau) = \frac{1}{N(1-T)}\left(1+\frac{\tau}{\tau_D}\right)^{-1}\left(1+\frac{\tau}{\beta^2\tau_D}\right)^{-1/2} \times \left(1-T+Te^{-\tau/\tau_T}\right)+1. \quad (12)$$

Here N is the average number of molecules in the detection volume; τ_D is the diffusion time, or the average passage time of a molecule through the volume; β is the ratio between the extension ($1/e^2$) of the sample volume in the axial and transverse direction, with the sample volume approximated as a three-dimensional Gaussian; T denotes the average fraction of molecules in the sample volume that are in the triplet state; and τ_T is their corresponding triplet relaxation time. Since the excitation intensity within the pulses was constant, τ_T was fixed to the value determined from the CW measurement (1.3 μs). The structure parameter

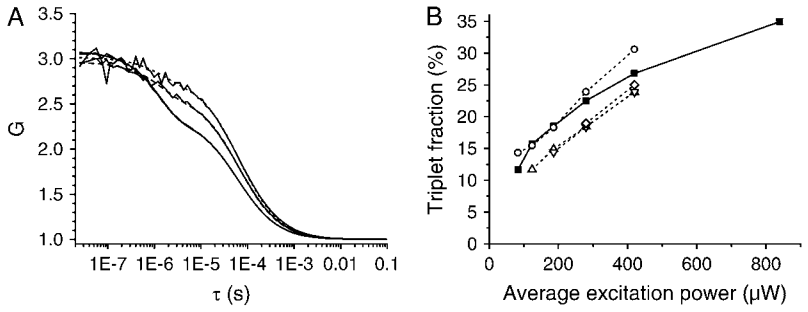

FIGURE 3 (*A*) Three measurements on the same Rh6G sample (*solid thin curves*) and their corresponding fits. The solid thick curve is a fit to the CW measurement, the thick dashed curve is a fit to the modulated measurement with 5.4-μs period and 900-ns pulse width ($n = 1$, $r = 1$), and the dotted curve is a fit to the modulated measurement with the same period and 100-ns pulse width ($n = 1$, $r = 3$). (*B*) Average fraction of molecules in the triplet state as a function of average excitation power for a sample of Rh6G. Note that average excitation power here refers to power averaged over the whole measurement, not only within an excitation pulse. The solid curve with solid squares shows data from a CW power series. The dashed curves connect measurements with the same modulation period, all having a constant peak power of 0.84 mW. The open circles represent a modulation series with 16.2-μs period and varying pulse widths, and hence varying duty cycles. Upward-pointing triangles signify 5.4 μs, downward-pointing triangles 1.8 μs, and diamonds 600-ns periods. Proper modulation provides more efficient triplet suppression than a corresponding decrease in excitation power.

β was fixed to 10 in all fits, based on results from calibration measurements with CW excitation. The approximation of the detection volume as a three-dimensional Gaussian is rather crude and gets worse the more the triplet state is populated. Triplet state population buildup introduces saturation effects (8,24,25) that are difficult to model with simple expressions. Therefore, the weighting of the data described by Eq. 11 was modified before application to the modulated measurements: All data points with lag times above 100 μs were assigned weights 100 times lower than the ones determined by Eq. 11 to focus the analysis on the part of the curves most strongly affected by the triplet kinetics and thus make the determination of the corresponding parameters as accurate as possible. The determination of the diffusion time is impeded by this procedure, but this parameter is not of interest in this case. For the same reason fits to data from CW measurements were done in an unweighted fashion.

Fig. 3 *B* shows that modulated excitation can be used to suppress triplet buildup more efficiently than can be achieved by decreasing excitation power. It can be seen that, as expected, the choice of modulation parameters is critical for optimal triplet suppression. After onset of excitation the triplet state is populated and the fluorescence intensity drops until steady state is reached. If the excitation is turned off before steady state is reached and the fluorophores are given time to relax back to the ground state before the onset of the next excitation pulse, the average triplet population is reduced. Optimally, the pulses should be so short, that fluorophores do not have the time to strongly accumulate in the triplet state, and the times between pulses should be long enough to allow sufficient relaxation back to the singlet ground state (12,16).

Protonation measurements on fluorescein

To show that modulated FCS can be used to separate processes overlapping in time, measurements were made on fluorescein at different pH. At the relevant pH values, fluorescein has two protonation forms: one nonprotonated dianionic form, which is fluorescent; and one protonated monoanionic form, which is very weakly fluorescent under the conditions of this study. Here we regard the latter form totally nonfluorescent, the only implication of which is a slight underestimation of the fraction of protonated dye in the sample. With this assumption, the protonation kinetics affect the correlation curve in exactly the same way as the triplet transitions. Further we assume that singlet-triplet transitions and protonation exchange take place independently. To determine the fraction of protonated dye, P, and the protonation relaxation time, τ_P, we used the model (11):

$$G(\tau) = \frac{1}{N(1-T)(1-P)}\left(1+\frac{\tau}{\tau_D}\right)^{-1}\left(1+\frac{\tau}{\beta^2\tau_D}\right)^{-1/2} \times \left(1-T+Te^{-\tau/\tau_T}\right)\left(1-P+Pe^{-\tau/\tau_P}\right)+1. \quad (13)$$

Lower pH means a higher concentration of protons available for reaction, increases the fraction of protonated fluorescein molecules, P, and makes the protonation process faster, which leads to a shortening of the protonation time, τ_P. Adding buffer speeds up the exchange and also shortens the protonation time, but leaves the protonation fraction unaffected. As a reference, measurements with both CW and modulated excitation were made on fluorescein in 10 mM phosphate buffer at pH 9.4, where essentially all molecules were in the unprotonated state and the correlation curves showed no protonation kinetics. Measurements were done at 84 μW excitation power. The triplet parameters were extracted by fitting Eq. 12 to the data, with weighting as for the Rh6G measurements (Fig. 4 *A*). There is a rather prominent dip in the correlation curve at the lag time corresponding to the pulse width of the modulation, due to the low number of photon pairs contributing to the correlation function for this particular lag time. As can be seen in the graph, thanks to the weighting, this dip hardly affects the fit. If necessary, the statistics can also be improved by slightly modifying the pulse trains.

Fig. 4 *B* shows corresponding measurements on a fluorescein sample with 1 mM phosphate buffer at pH 6.0. This pH gives prominent protonation, and the buffer concentration was chosen such that the protonation time is

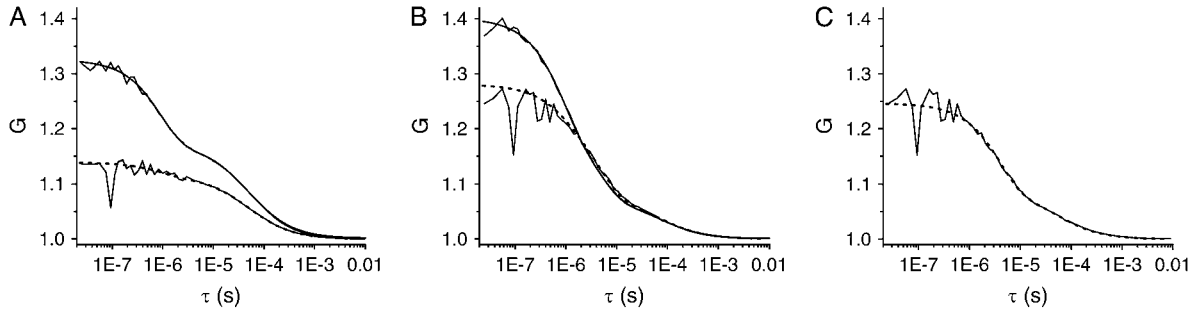

FIGURE 4 (*A*) Measurements on fluorescein in 10 mM phosphate buffer at pH 9.4 with 84 μW excitation power. No protonation is assumed due to the high pH. A global fit of Eq. 12 with the triplet relaxation time as common variable, the structure factor β fixed to 10 and all other parameters free is shown as a solid line for the CW measurement and as a dashed line for the modulated measurement with 5.4-μs period and 100-ns pulse width ($n = 1$, $r = 3$). The fit gives a triplet relaxation time of 0.94 μs and triplet fractions of 48% and 18%, respectively. (*B*) Measurements on fluorescein in 1 mM phosphate buffer at pH 6.0 performed in the same manner as presented in panel *A*. A global fit of Eq. 13, with protonation time and fraction as common variables, triplet parameters fixed to the results achieved in panel *A*, the structure factor β fixed to 10, and all other parameters free, indicates 66% protonated dye with protonation time 5.0 μs. (*C*) The same modulated measurement as in panel *B* but fit with a model assuming no triplet (Eq. 13 with T fixed to 0, τ_T to an arbitrary value, β to 10, and all other parameters free). This gives a protonation fraction of 64% and a protonation time of 4.2 μs.

very close to the triplet time, making the two processes hard to separate. A global fit of Eq. 13, with triplet parameters fixed to the values achieved for the measurements at pH 9.4 and protonation parameters as common variables, gave a fraction of protonated species of 66% and a protonation time of 5.0 μs.

The measurement with modulated excitation in Fig. 4 *B* is depicted again in Fig. 4 *C*, but this time with a fit assuming zero triplet population. This yields protonation fraction and time of 64% and 4.2 μs, which compares well with the values from above. A lower excitation power would help reduce the triplet influence even further. This indicates that modulated excitation can suppress the triplet population to the extent that triplet kinetics need not be taken into account in the FCS analysis anymore.

CONCLUDING REMARKS

In this work, a concept is introduced and experimentally verified for how distortion-free correlation data can be obtained over the full correlation timescale in FCS experiments with modulated excitation. The possibility to apply modulated excitation in FCS experiments brings several advantages. The introduction of excitation modulation in FCS provides a new set of parameters for optimizing the photophysical conditions for a measurement. Here it has been shown that modulated excitation can be used to suppress triplet population buildup more efficiently than by reducing the CW excitation power. This results in higher fluorescence intensity during excitation and reduced photobleaching. Further, it is demonstrated how suppression of the triplet state, or any other photoinduced state, in excitation-modulated FCS experiments can offer more robust data analysis and interpretation thanks to the added possibilities to separate processes from each other. Apart from the benefits that follow from the possibility to suppress the population of long-lived photoinduced states, several additional applications deserve to be pointed out, where full correlation timescale FCS data may be needed, and where modulated excitation is either necessary or brings specific advantages. First, the possibility to perform FCS experiments with modulated excitation adds the option of applying time gating to improve the signal/background ratio under conditions with stray light or high dark current. Under the conditions of this study this brings no advantage but it will prove useful for measurements of molecules with long dwell times in the FCS detection volume. Pulsed illumination, for both one- and two-photon excitation, has previously been suggested in this context (26,27) where a continuous excitation would tend to bleach the molecules before their exit out of the excitation volume. Further, various excitation schemes yielding photoinduced off-switching of fluorescence have proven useful for breaking the diffraction barrier in fluorescence microscopy (28,29). The possibility to combine these concepts with fluctuation spectroscopy and FCS also offers the possibility to reduce the size of the detection volume significantly. This has been demonstrated using stimulated emission as a switch-off mechanism of the fluorescence (30). The work presented here also demonstrates that several other, experimentally more easily realizable switching mechanisms can be combined with FCS measurements, no matter what the time range of the switching mechanism is. Taken together, the approach described and verified in this work will prove very useful in a range of applications, where full correlation timescale FCS data is needed, and where the use of modulated excitation can provide distinctive advantages.

APPENDIX I: DERIVATION OF WEIGHTING FUNCTION

The correlation function $G(\tau)$ can be regarded a function of the number of photon pairs $N_p(\tau)$ occurring separated by a time within an interval around τ, and the total number of photons in each detection channel, N_1 and N_2, contributing to the correlation function:

$$G(\tau) = A\frac{N_p(\tau)}{N_1 N_2}. \quad \text{(A1)}$$

A is here a proportionality constant depending on the binning of the correlation function. Introducing indices D and S in Eq. A1 to denote the direct and the shifted correlation functions, respectively, we can express the filtered correlation function as a ratio of the two:

$$G_F(\tau) = \frac{G_D(\tau)}{G_S(\tau)} = \frac{N_{p,D}(\tau)}{N_{1,D}N_{2,D}} \cdot \frac{N_{1,S}N_{2,S}}{N_{p,S}(\tau)}. \quad \text{(A2)}$$

The proportionality constant cancels out, since both correlation functions must be calculated in the same way. Assuming that all $N_{i,j}$ are generated by independent Poissonian processes we can approximate their standard deviations:

$$\sigma\left[N_{i,j}\right] = \sqrt{\langle N_{i,j}\rangle} \approx \sqrt{N_{i,j}}. \quad \text{(A3)}$$

Here the expectation value $\langle N_{i,j}\rangle$ is approximated by the measured $N_{i,j}$ and propagation of errors gives:

$$\sigma[G_F(\tau)] = G_F(\tau)\sqrt{\sum_{i,j}\frac{\sigma^2[N_{i,j}]}{N_{i,j}^2}} \approx G_F(\tau)\sqrt{\sum_{i,j}\frac{1}{N_{i,j}}}. \quad \text{(A4)}$$

The authors thank Dr. Anders Hedqvist for valuable discussions and Dr. Hans Blom for manuscript proofreading.

This work was financially supported by the Swedish National Research Council (VR-NT), the European Union (6FP, New and Emerging Science and Technology—SPOTLITE), and the Royal Institute of Technology (KTH).

REFERENCES

1. Magde, D., E. Elson, and W. W. Webb. 1972. Thermodynamic fluctuations in a reacting system—measurement by fluorescence correlation spectroscopy. *Phys. Rev. Lett.* 29:705–708.
2. Rigler, R., and E. Elson. 2001. Fluorescence Correlation Spectroscopy—Theory and Applications. F. P. Schafer, J. P. Toennies, and W. Zinth, editors. Springer-Verlag, Berlin, Germany.
3. Widengren, J., and Ü. Mets. 2002. Conceptual basis of fluorescence correlation spectroscopy and related techniques as tools in bioscience. *In* Single Molecule Detection in Solution, Methods and Applications, 1st Ed. C. Zander, J. Enderlein, and R. A. Keller, editors. Wiley-VCH Verlag, Berlin, Germany. 69–120.
4. Schwille, P., and E. Haustein. 2002. Fluorescence correlation spectroscopy, an introduction to its concepts and applications. *In* Single Molecule Techniques. P. Schwille, editor. Biophysical Society, Bethesda, MD.
5. Krichevsky, O., and G. Bonnet. 2002. Fluorescence correlation spectroscopy: the technique and its applications. *Rep. Prog. Phys.* 65:251–297.
6. Thompson, N. L., A. M. Lieto, and N. W. Allen. 2002. Recent advances in fluorescence correlation spectroscopy. *Curr. Opin. Struct. Biol.* 12:634–641.
7. Hess, S. T., S. H. Huang, A. A. Heikal, and W. W. Webb. 2002. Biological and chemical applications of fluorescence correlation spectroscopy: a review. *Biochemistry.* 41:697–705.
8. Widengren, J., Ü. Mets, and R. Rigler. 1995. Fluorescence correlation spectroscopy of triplet-states in solution—a theoretical and experimental study. *J. Phys. Chem.* 99:13368–13379.
9. Widengren, J., and P. Schwille. 2000. Characterization of photoinduced isomerization and back-isomerization of the cyanine dye Cy5 by fluorescence correlation spectroscopy. *J. Phys. Chem. A.* 104:6416–6428.
10. Widengren, J., J. Dapprich, and R. Rigler. 1997. Fast interactions between Rh6G and dGTP in water studied by fluorescence correlation spectroscopy. *Chem. Phys.* 216:417–426.
11. Widengren, J., B. Terry, and R. Rigler. 1999. Protonation kinetics of GFP and FITC investigated by FCS—aspects of the use of fluorescent indicators for measuring pH. *Chem. Phys.* 249:259–271.
12. Sandén, T., G. Persson, P. Thyberg, H. Blom, and J. Widengren. 2007. Monitoring kinetics of highly environment sensitive states of fluorescent molecules by modulated excitation and time-averaged fluorescence intensity recording. *Anal. Chem.* 79:3330–3341.
13. Song, L. L., C. Varma, J. W. Verhoeven, and H. J. Tanke. 1996. Influence of the triplet excited state on the photobleaching kinetics of fluorescein in microscopy. *Biophys. J.* 70:2959–2968.
14. Eggeling, C., J. Widengren, R. Rigler, and C. A. M. Seidel. 1998. Photobleaching of fluorescent dyes under conditions used for single-molecule detection: evidence of two-step photolysis. *Anal. Chem.* 70:2651–2659.
15. Widengren, J., A. Chmyrov, C. Eggeling, P.-Å. Löfdahl, and C. A. M. Seidel. 2007. Strategies to improve photostabilities in ultrasensitive fluorescence spectroscopy. *J. Phys. Chem. A.* 111:429–440.
16. Donnert, G., C. Eggeling, and S. W. Hell. 2007. Major signal increase in fluorescence microscopy through dark-state relaxation. *Nat. Methods.* 4:81–86.
17. Hanbury Brown, R., and R. Q. Twiss. 1956. Correlation between photons in two coherent beams of light. *Nature.* 177:27–29.
18. Koppel, D. E. 1974. Statistical accuracy in fluorescence correlation spectroscopy. *Phys. Rev. A.* 10:1938–1945.
19. Saleh, B. 1978. Photoelectron Statistics: With Applications to Spectroscopy and Optical Communication. Springer-Verlag, Berlin, Germany and New York.
20. Laurence, T. A., S. Fore, and T. Huser. 2006. Fast, flexible algorithm for calculating photon correlations. *Opt. Lett.* 31:829–831.
21. Eggeling, C., S. Berger, L. Brand, J. R. Fries, J. Schaffer, A. Volkmer, and C. A. M. Seidel. 2001. Data registration and selective single-molecule analysis using multi-parameter fluorescence detection. *J. Biotechnol.* 86:163–180.
22. Gregor, I., D. Patra, and J. Enderlein. 2005. Optical saturation in fluorescence correlation spectroscopy under continuous-wave and pulsed excitation. *ChemPhysChem.* 6:164–170.
23. Widengren, J., R. Rigler, and Ü. Mets. 1994. Triplet-state monitoring by fluorescence correlation spectroscopy. *J. Fluoresc.* 4:255–258.
24. Enderlein, J., I. Gregor, D. Patra, T. Dertinger, and U. B. Kaupp. 2005. Performance of fluorescence correlation spectroscopy for measuring diffusion and concentration. *ChemPhysChem.* 6:2324–2336.
25. Hess, S. T., and W. W. Webb. 2002. Focal volume optics and experimental artifacts in confocal fluorescence correlation spectroscopy. *Biophys. J.* 83:2300–2317.
26. Weissman, M., H. Schindler, and G. Feher. 1976. Determination of molecular weights by fluctuation spectroscopy: application to DNA. *Proc. Natl. Acad. Sci. USA.* 73:2776–2780.
27. Berland, K. M., P. T. C. So, Y. Chen, W. W. Mantulin, and E. Gratton. 1996. Scanning two-photon fluctuation correlation spectroscopy: particle counting measurements for detection of molecular aggregation. *Biophys. J.* 71:410–420.
28. Hell, S. W. 2003. Toward fluorescence nanoscopy. *Nat. Biotechnol.* 21:1347–1355.
29. Hofmann, M., C. Eggeling, S. Jakobs, and S. W. Hell. 2005. Breaking the diffraction barrier in fluorescence microscopy at low light intensities by using reversibly photoswitchable proteins. *Proc. Natl. Acad. Sci. USA.* 102:17565–17569.
30. Kastrup, L., H. Blom, C. Eggeling, and S. W. Hell. 2005. Fluorescence fluctuation spectroscopy in subdiffraction focal volumes. *Phys. Rev. Lett.* 94:178104.